


Transcriptional profile changes caused by noise-induced tinnitus in the cochlear nucleus and inferior colliculus of the rat

Xinmiao Xue^{a,b,c,d} , Peng Liu^{a,b,c,d}, Chi Zhang^{b,c}, Zhiwei Ding^{a,b,c}, Li Wang^{a,b,c}, Yuke Jiang^{a,b,c}, Wei-dong Shen^{b,c}, Shiming Yang^{a,b,c,d} and Fangyuan Wang^{a,b,c,d}

^aThe Six Medical Center, PLA General Hospital, Beijing, PR China; ^bMedical School of Chinese PLA, Beijing, PR China; ^cDepartment of Otolaryngology, Head and Neck Surgery, Institute of Otolaryngology, Chinese PLA General Hospital, Beijing, PR China; ^dNational Clinical Research Center for Otolaryngologic Diseases, Beijing, PR China

ABSTRACT

Introduction: Tinnitus is a prevalent and disabling condition characterized by the perception of sound in the absence of external acoustic stimuli. The hyperactivity of the auditory pathway is a crucial factor in the development of tinnitus. This study aims to examine genetic expression variations in the dorsal cochlear nucleus (DCN) and inferior colliculus (IC) following the onset of tinnitus using transcriptomic analysis. The goal is to investigate the relationship between hyperactivity in the DCN and IC.

Methods: To confirm the presence of tinnitus behavior, we utilized the gap pre-pulse inhibition of the acoustic startle (GPIAS) response paradigm. In addition, we conducted auditory brainstem response (ABR) tests to determine the baseline hearing thresholds, and repeated the test one week after subjecting the rats to noise exposure (8–16 kHz, 126 dBHL, 2 h). Samples of tissue were collected from the DCN and IC in both the tinnitus and non-tinnitus groups of rats. We employed RNA sequencing and quantitative PCR techniques to analyze the changes in gene expression between these two groups. This allowed us to identify any specific genes or gene pathways that may be associated with the development or maintenance of tinnitus in the DCN and IC.

Results: Our results demonstrated tinnitus-like behavior in rats exposed to noise, as evidenced by GPIAS measurements. We identified 61 upregulated genes and 189 downregulated genes in the DCN, along with 396 upregulated genes and 195 downregulated genes in the IC. Enrichment analysis of the DCN revealed the involvement of ion transmembrane transport regulation, synaptic transmission, and negative regulation of neuron apoptotic processes in the development of tinnitus. In the IC, the enrichment analysis indicated that glutamatergic synapses and neuroactive ligand-receptor interaction pathways may significantly contribute to the process of tinnitus development. Additionally, protein-protein interaction (PPI) networks were constructed, and 9 hub genes were selected based on their betweenness centrality rank in the DCN and IC, respectively.

Conclusions: Our findings reveal enrichment of differential expressed genes (DEGs) associated with pathways linked to alterations in neuronal excitability within the DCN and IC when comparing the tinnitus group to the non-tinnitus group. This indicates an increased trend in neuronal excitability within both the DCN and IC in the tinnitus model rats. Additionally, the enriched signaling pathways within the DCN related to changes in synaptic plasticity suggest that the excitability changes may propagate to IC.

New and Noteworthy: Our findings reveal gene expression alterations in neuronal excitability within the DCN and IC when comparing the tinnitus group to the non-tinnitus group at the transcriptome level. Additionally, the enriched signaling pathways related to changes in synaptic plasticity in the differentially expressed genes within the DCN suggest that the excitability changes may propagate to IC.


ARTICLE HISTORY

Received 19 May 2024
Revised 19 May 2024
Accepted 23 May 2024

KEYWORDS

Tinnitus; dorsal cochlear nucleus; inferior colliculus; transcriptional profile; and neuronal hyperactivity

CONTACT Fangyuan Wang  fangyuanwang05@163.com; Shiming Yang  shm_yang@163.com  Department of Otolaryngology, Head and Neck Surgery, Institute of Otolaryngology, Chinese PLA General Hospital, Beijing 100853, PR China

 Supplemental data for this article can be accessed online at <https://doi.org/10.1080/07853890.2024.2402949>.

© 2024 The Author(s). Published by Informa UK Limited, trading as Taylor & Francis Group

This is an Open Access article distributed under the terms of the Creative Commons Attribution-NonCommercial License (<http://creativecommons.org/licenses/by-nc/4.0/>), which permits unrestricted non-commercial use, distribution, and reproduction in any medium, provided the original work is properly cited. The terms on which this article has been published allow the posting of the Accepted Manuscript in a repository by the author(s) or with their consent.

Introduction

Subjective tinnitus, characterized by the perception of sound attributed to a location inside the head, to both ears, or to one ear without an external acoustic trigger, is a common and debilitating condition that affects many individuals. Recent research has significantly contributed to our understanding of the changes in auditory and non-auditory brain structures associated with tinnitus [1–4]. These studies have provided valuable insights into the mechanisms underlying tinnitus and its impact on the overall well-being of individuals. However, the clinical treatment outcomes for tinnitus remain less than ideal due to the unclear understanding of its pathogenesis.

There are several hypotheses about the mechanism of tinnitus processes, including prediction error in the auditory system [1], resetting of sensory predictions [2], and dysfunction of the ‘noise-cancellation system’ [3]. Moreover, tinnitus has been hypothesized to be a consequence of the compensatory responses in the central auditory system to decreased peripheral input resulting from hearing loss [4,5], which was named the central gain mechanism [6,7]. Even patients with tinnitus, who do not suffer from overt hearing loss, could have ‘hidden hearing loss’ [8,9], which was defined as the auditory dysfunction unsuccessfully revealed by standard tests of auditory thresholds, and characterized by cochlear synaptopathy influencing the afferent signal of the inner hair cells [10]. And in previous animal studies, it has been illustrated that tinnitus may be the result of a synaptopathy at the inner hair cells independent of hidden or clinical relevant hearing [11,12]. Moreover, reduced auditory nerve activity within the peripheral system after acoustic overexposure has been previously reported [13,14]. As a compensatory mechanism, DCN may exhibit hyperactivity, which can manifest as increased synchrony and bursting of neural activity [5,15]. The role of the DCN in the pathophysiology of tinnitus has been emphasized in previous studies, as it serves as the primary location where multiple sensory inputs converge in the auditory pathway [7,16–18]. Animal studies have indeed shown that a functioning DCN is necessary for the development of tinnitus [19]. By manipulating the DCN or its related neural pathways, researchers have observed changes in tinnitus perception or its associated neural activity in animal models [7,20]. The abnormal neural activity in the DCN can propagate through the auditory pathway and impact the functioning of the upstream areas, including the IC [21,22], the medial geniculate body of the thalamus [23] and the primary auditory cortex [24,25].

Moreover, several animal studies have reported that IC hyperactivity is also related to tinnitus [26–28]. Multiformal similar neuronal plasticity changes have been observed in the IC [29], including an increasing number of neuronal bursting [26] and a variation in the response mode from ‘sustained’ to ‘onset firing’ [30]. However, there are two possible ways in which IC neuronal excitability may change: one is through passive reception of increased excitatory input from DCN, and the other is through compensatory adjustments in local regions [31]. Currently, it is not yet clear how these two mechanisms contribute to the increased excitability of neurons in IC. Furthermore, there have been relatively few studies investigating gene expression changes in DCN and IC.

Consequently, the purpose of this study is to investigate the genetic expression variations of tinnitus in DCN and IC by utilizing transcriptomic analysis. We performed RNA-seq integrated with bioinformatics to uncover DEGs in the DCN of rats with or without noise-induced tinnitus after noise exposure to screen for possible signaling pathways and potential genes that contribute to the underlying mechanism of tinnitus.

2. Materials and methods

2.1. Animals

The animal experiments in this study were conducted in accordance with the guidelines for the Care and Use of Laboratory Animals of the Chinese PLA General Hospital (SQ2021284). The study adhered to the ARRIVE guidelines. Only two-month-old male rats (weighing between 200–250 g) were included in this study, while female rats were excluded because of the consideration about the variable amplitude of the startle reflex during the estrous cycle [32,33]. And the rats were randomly divided into sham noise exposure and noise exposure groups by the SPSS software. They were all housed in standard cages and provided with sufficient water and food under a 12-hour light/dark cycle. The experimental design process is shown in [Figure 1A](#). The rats were acclimatized for one week prior to the study. The entire experimental protocol was approved by the Chinese PLA General Hospital Animal Ethics Committee. There were 8 rats in each group, and a total 24 animals were used in this study. The required experimental animal size was calculated according to the resource equation method [34]. Detail methodology can be found in [Supplementary Data 1](#). No rat was excluded during the whole study. For the RNA-seq analysis, three rats were included in both the tinnitus

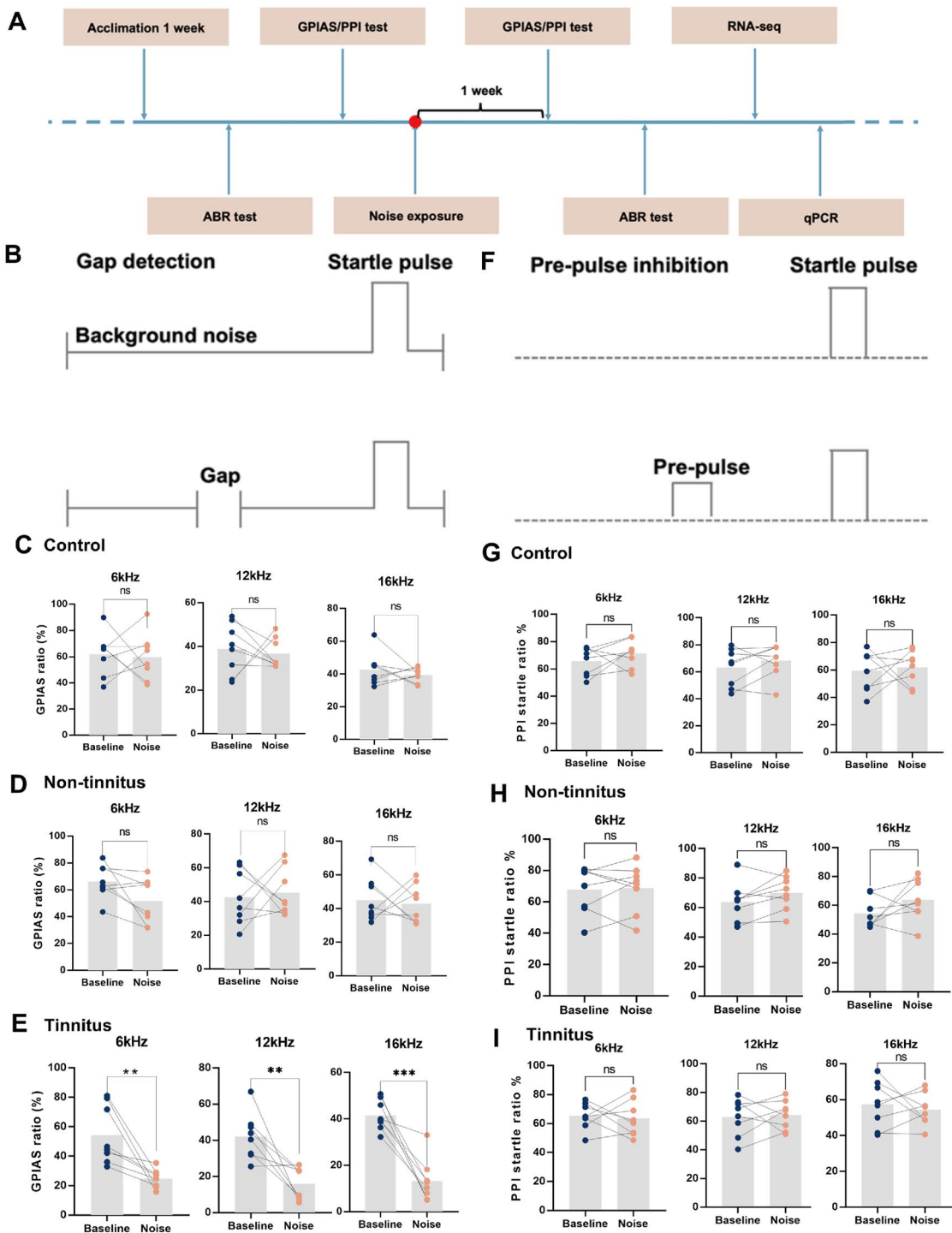


Figure 1. Gap detection and pre-pulse inhibition performance at different frequencies measured before and after noise exposure. (A) Diagram illustrating the process to establish a noise-induced tinnitus animal model. (B) Schematic view of GPIAS. Summary graph of GPIAS ratio (1-response to gap and startle stimulus/response to startle alone) for three different frequencies of background for (C) control, (D) non-tinnitus and (E) tinnitus groups. There was no significant difference in GPIAS ratio between before and after noise exposure in both the control and the non-tinnitus groups, while the GPIAS ratio was significantly decreased in tinnitus rats because the potential tinnitus noise frequency may fill the silent gap after noise exposure. (F) Schematic view of pre-pulse inhibition (PPI) of the acoustic startle reflex. Summary graph of PPI startle ratio (1-response to pre-pulse and startle stimulus/response to startle alone) with different frequencies of pre-pulse for (G) control, (H) non-tinnitus and (I) tinnitus groups. In the three groups, there was no significant difference in PPI ratio before and after noise exposure. ($n=8$, ** indicates $p < .01$, *** indicates $p < .001$).

and non-tinnitus groups, while five rats were used for the quantitative PCR (qPCR) experiment in each group.

2.2. Auditory brainstem responses (ABR)

In order to investigate the hearing loss effects of noise exposure, ABR thresholds were measured one week before and one week after noise exposure by an observer without knowing the group of rats. To maintain anesthesia, rats were injected with pentobarbital sodium (40 mg/kg) and placed in a soundproof chamber with a warming blanket. Subcutaneous metallic needle electrodes were inserted at the vertex (non-inverting input), behind the stimulated ear (inverting input), and behind the non-stimulated ear (ground). To deliver tone and click stimuli, a TDT loudspeaker connected to a TDT RZ6 instrument was inserted into the external auditory canal *via* a tube. The multifunction processor (RX6, TDT) was used to generate clicks and tone bursts at frequencies of 4, 8, 16, and 32 kHz for ABR induction in the rats. The click stimulus consisted of a burst of white noise with energy ranging from 0.8 to 43 kHz [35]. The initial stimulus intensity of 90 dB was gradually decreased in 10 dB increments until no response was observed. Following this, the stimulus intensity was adjusted in increments of 5 dB, either increasing or decreasing based on the absence of response. The ABR threshold was determined as the lowest dB SPL at which repeatable waveforms were present. The responses were recorded during the procedure and subsequently analyzed using computer software.

2.3. Gap detection

We conducted a gap-induced prepulse inhibition of the acoustic startle response (GPIAS) experiment before and one week after noise exposure to investigate whether rats develop tinnitus following exposure to noise, as described in a recent study [36]. In brief, rats were placed in a cage equipped with a piezoelectric sensor that detected pressure changes caused by the startle reflex and rapidly converted them into voltage signals. In the 'no gap' trials, a startle stimulus (115 dB SPL, 50 ms) was presented in the presence of narrowband background noise (6, 12, and 16 kHz) at 60 dB SPL. The 'gap' trials involved inserting a silent gap (50 ms) before the startle stimulus, as shown in Figure 1B. The testing order of the 10 paired 'gap' and 'no gap' trials was randomized. The performance of gap detection was evaluated by calculating the GPIAS ratio, which is calculated by '1-gap acoustic startle response amplitude/no gap acoustic startle response

amplitude'. In normal rats, the acoustic startle reflex is attenuated when a silent gap is introduced within the continuous background noise. However, in rats with tinnitus, there would be no obvious inhibition presented as the potential tinnitus noise frequency fills the silent gap. As not all noise-exposed rats develop tinnitus [28,37], we used a GPIAS ratio below 30% in at least one frequency (6, 12, or 16 kHz) as the criterion for tinnitus, aligning with previous research [38–40]. We measured the GPIAS ratio before and one week after sham or noise exposure to evaluate changes. Rats in both sham noise exposure and noise exposure groups were interspersed for experiments to exclude confounding factors caused by the tested order. Based on the results, the study comprised three groups: the control group (sham noise exposure), the tinnitus group (exposed to noise with tinnitus-like behavior), and the non-tinnitus group (exposed to noise without tinnitus-like behavior). Gap detection deficits were evaluated using the Xeye hardware and software (Beijing, China).

2.4. Prepulse inhibition (PPI)

PPI testing was conducted in conjunction with the gap detection testing, both before and one week after sham or noise exposure. The PPI testing involved prepulse trials and startle-only trials, as depicted in Figure 1F. During the prepulse trials, a prepulse sound with a similar intensity to the background sound used in the gap detection test was presented (50 ms, 70 dB bandpass sound with a 1 kHz bandwidth centered at 6, 12, and 16 kHz). The prepulse preceded the startle stimulus by 100 ms. The startle-only trials were similar to the prepulse trials, but no prepulse sound was delivered. The PPI ratio, calculated as '1-prepulse response amplitude/startle-only response amplitude', was utilized to assess the performance of rats.

2.5. Noise exposure

After all rats were anesthetized with pentobarbital sodium (40 mg/kg) intraperitoneal injection, the earplugs were unilaterally inserted in their right ears to ensure that the rats retained normal hearing in the unilateral ear specifically for gap detection [41]. Following that, the rats both in the tinnitus group and non-tinnitus group were subjected to a 2-hour exposure of wideband noise spanning from 8 to 16 kHz with a sound pressure level (SPL) of 126 dBHL, while the control group underwent the same procedure as the two groups above except without noise exposure. The intense noise was generated using a sophisticated attenuator (PA5 TDT, Alachua,

FL, USA) and amplified through an MF-1201 MOSTET amplifier (ATech). It was then emitted from a rounded loudspeaker (Aijie Audio Equipment Factory), positioned at a distance of 10cm from the left ear of the rats. The noise level was accurately calibrated using a sound level meter (Brüel & Kjær, 2250L, Denmark), along with a pre-amplifier (RA4PA, 4-channel, TDT) and a condenser microphone (RA4LI, TDT).

2.6. RNA-seq

One week after exposure to noise, rats were anesthetized with pentobarbital sodium (40mg/kg). While under deep anesthesia, their brains were removed and tissue samples from both the tinnitus and non-tinnitus groups ($n=3$) were collected from DCN and IC. The samples were promptly preserved in TRIzol reagent (Thermo Fisher Scientific). The quality and concentration of the RNA were assessed using a NanoDrop 2000 instrument (Thermo Fisher Scientific) in Wilmington, DE, USA. RNA integrity was evaluated using an RNA Nano 6000 Assay Kit on an Agilent Bioanalyzer 2100 System (Agilent Technologies) in CA, USA. The NEBNext Ultra™ RNA Library Prep Kit for Illumina (NEB, USA) was used to generate sequencing libraries, with index codes added for sample identification. Raw reads were processed using in-house Perl scripts, which involved the removal of poly-N-containing reads, adapters, and low-quality reads to obtain clean data. Metrics such as Q20, Q30, GC content, and sequence duplication levels were calculated for the cleaned data. Comprehensive downstream analyses were conducted using high-quality clean data.

2.7. Bioinformatics analysis

Differential expression analysis of the DCN tissue samples was performed using EdgeR. Significant differential expressions were defined with p values $<.05$ and a fold change ≥ 1.5 . GSeq R package and KOBAS software were utilized for GO and KEGG enrichment

analyses, respectively. The protein-protein interaction (PPI) network was constructed by inputting the DEGs into the STRING database (<http://stringdb.org/>) [42]. The medium confidence level (0.400) and the highest confidence level (0.900) of the interaction score were used to respectively determine the statement for identifying each connection [43]. The plug-in named CytoNCA at Cytoscape software was used to rank the highly connected genes in the PPI network (obtained in the medium confidence level (0.400)) based on betweenness centrality (BC) [44]. The top nine genes were selected as the hub genes in this study.

2.8. Quantitative polymerase chain reaction (qPCR)

One week after exposure to noise, the rats were anesthetized with pentobarbital sodium at a dose of 40mg/kg, and their brains were removed following decapitation. Total RNA was extracted from DCN and IC tissue samples using an RNA extraction reagent (Servicebio, Wuhan, China), and then converted into complementary DNA (cDNA) using the Servicebio®RT First Strand cDNA Synthesis Kit (Servicebio, Wuhan, China). For qPCR, a 2×SYBR Green qPCR Master Mix (Servicebio, Wuhan, China) was utilized. The mRNA levels of GAPDH or β -actin were employed as a reference to normalize the mRNA levels of the chosen genes, and the $2^{-\Delta\Delta CT}$ method was applied to determine the fold change in gene expression. The oligonucleotide primers (Servicebio, Wuhan, China) used in this study are listed in Tables 1 and 2.

2.9. Statistics

All data were analyzed using GraphPad Prism software (version 9.0.1, San Diego, CA, USA). We adopted a mean \pm SEM pattern to depict the data and performed a Student's t-test to analyze normally distributed data in this study. A paired t-test was used to analyze the GPIAS ratio and PPI ratio before and after noise exposure. The ABR thresholds were assessed using two-way

Table 1. Primer sequence of genes selected from DEGs in DCN for qPCR analysis.

| Genes | Forward | Reverse |
|----------------|--------------------------|-------------------------|
| <i>Calb1</i> | GGAATCAAATGTGTGGGAAAGAG | AGGCTTTTCAGTAAGGCATCCAG |
| <i>Fos</i> | TCCAAGCGGAGACAGATCAACT | TCAAGTCCAGGGAGGTCACAGA |
| <i>Grid2</i> | CTCACCAGGAGCAACAGAAACG | CCTCATGGGTGCAAAAGAGCGTG |
| <i>Rgs8</i> | TGATGCCACGCAGGAACAAA | AAGGAATCTGCCACCTCGTC |
| <i>Hpcal4</i> | GAGATGCTGGAGATCATTGAGGC | TCCTTGAATCCTCCAGCGTAAT |
| <i>Sdc1</i> | AGGTGCTTTGCCAGATATGACTTT | GTATCCCTGCTGGTGGTTCT |
| <i>Cacna1a</i> | GACACGGCCTTACTTCCACTCT | CTCGTAACACGCTGATTCCAAA |
| <i>Gria1</i> | GAATCAGAACGCCTCAACGC | TGTCACATTGGCTCCGCTCT |
| <i>Itpr1</i> | CGAATGGATTTATCAGCACCTT | ACCGCATCTGTTGACTGTTGG |
| <i>Nos1</i> | TCATCCATTAAGAGATTGGCTCC | GTGGCATACTGACATGGTTACAG |
| <i>GAPDH</i> | CTGGAGAAACCTGCCAAGTATG | GGTGAAGAATGGGAGTTGCT |

Table 2. Primer sequence of genes selected from DEGs in IC for qPCR analysis.

| Genes | Forward | Reverse |
|----------------|--------------------------|--------------------------|
| <i>Jup</i> | AGCAACAAGCCTGCCATCGT | CAGGATCTTCAGCACGTTCTCC |
| <i>Prkcg</i> | ACAGGGACCTCAAGTTGGATAATG | TCCCATAGGGCTGATAGGCAAT |
| <i>Fos</i> | TCCAAGCGGAGACAGATCAACT | TCAAGTCCAGGGAGGTCACAA |
| <i>Sdc1</i> | AGGTGCTTTGCCAGATGACTTT | GTATCCCTGTGGTGGGTTCT |
| <i>Itgb4</i> | ATCTTTGCCGTACCAACTACTCT | GATAGAAAAGCCTCCTCCAGCA |
| <i>Pax6</i> | ACATCCCTATCAGCAGCAGTTTC | GTATCATAACTCCGCCCATCA |
| <i>Kit</i> | ATCAGGGCGACTTCAATTACG | CTGCTGGTTCAGGTTTAGGG |
| <i>Daw1</i> | ATGCTGTGGGATGTACAAGTG | GCAATAAGTTTCCCAGTGTAGCAA |
| <i>USH2A</i> | TGAATCCTGAAGCCACCT | CTGGAGAACCGAATGGTGATTT |
| β -actin | TGCTATGTTGCCCTAGACTTCG | GTTGGCATAGAGGTCTTTACGG |

ANOVA. p -values less than .05 were considered statistically significant.

3. Results

3.1. Establishment of noise-induced tinnitus in rats

We evaluated the ABR, GPIAS ratio, and PPI ratio at both baseline and one week post-noise exposure (refer to Figure 1A). In the GPIAS tests (Figure 1B), the control group and non-tinnitus groups did not show any significant changes in their gap detection performance after noise exposure when the gaps were embedded in background sound filtered at frequencies of 6, 12, and 16 kHz (Figure 1C,D). In contrast, the gap inhibition was evident in tinnitus group at all three frequencies (Figure 1E). Additionally, to eliminate the potential impacts of hyperacusis and hypoacusis caused by noise exposure, PPI tests were also conducted (Figure 1F). The results showed no notable variations in the PPI ratio between the pre- and post-noise exposure stages across all experimental groups, including control, non-tinnitus and tinnitus groups (Figure 1G–I). The values of the GPIAS ratio and PPI ratio among the three groups were also exhibited in Table S1. Meanwhile, the ABR threshold in the left ear was significantly increased after noise exposure (Figure 2A). Both tinnitus and the non-tinnitus groups demonstrated parallel changes in ABR thresholds after noise exposure. Specifically, there was a marked elevation at all frequencies in the left ears, while effective hearing protection was observed in the right ears among both groups (Figure 2B,C). Table S2 listed the values of ABR threshold of rats before and after noise exposure.

3.2. The identification of genes that expressed differently in both DCN and IC between the tinnitus group and the non-tinnitus group

We employed RNA-seq analysis technology to examine the changes in gene expression in DCN and IC tissues of rats across tinnitus and non-tinnitus groups.

Differential expression analysis was performed to identify genes with a fold change greater than 1.5 between the tinnitus and non-tinnitus groups, leading to the discovery of 61 upregulated genes and 189 downregulated genes in the DCN, as well as 396 upregulated genes and 195 downregulated genes in the IC. The differential expression of genes is visually represented in the heatmap (Figures S1 and S2) and volcano plot (Figure 3A,B), where upregulated genes are indicated in red and downregulated genes are indicated in blue. And we have presented the top 10 upregulated and downregulated genes in the DCN (Table 3) and IC (Table 4) regions

3.3. DEGs enrichment analysis in DCN and IC

The biological functions of the DEGs of DCN were determined using gene ontology (GO) enrichment analysis. Significantly enriched terms in the categories of biological process (BP), cellular components (CC), and molecular function (MF) are displayed in Figure 4A–C. The top five terms in the BP ontology were regulation of ion transmembrane transport, synaptic transmission, glutamatergic, negative regulation of neuron apoptotic process, homophilic cell adhesion *via* plasma membrane adhesion molecules, and long-term memory (Figure 4A). The most enriched CC process was glutamatergic synapse, followed by neuronal cell body, voltage-gated potassium channel complex, presynaptic membrane, and dendritic spine membrane (Figure 4B). In the MF process, the top five enriched terms were voltage-gated potassium channel activity, calcium ion binding, Wnt-protein binding, Wnt-activated receptor activity, and purinergic nucleotide receptor activity (Figure 4C). To further explore the underlying pathways involving the DEGs between the tinnitus and non-tinnitus groups, KEGG analysis was conducted and the potential pathways identified were long-term depression, ECM-receptor interaction, spinocerebellar ataxia, phosphatidylinositol signaling system, and protein digestion and absorption (Figure 4D).

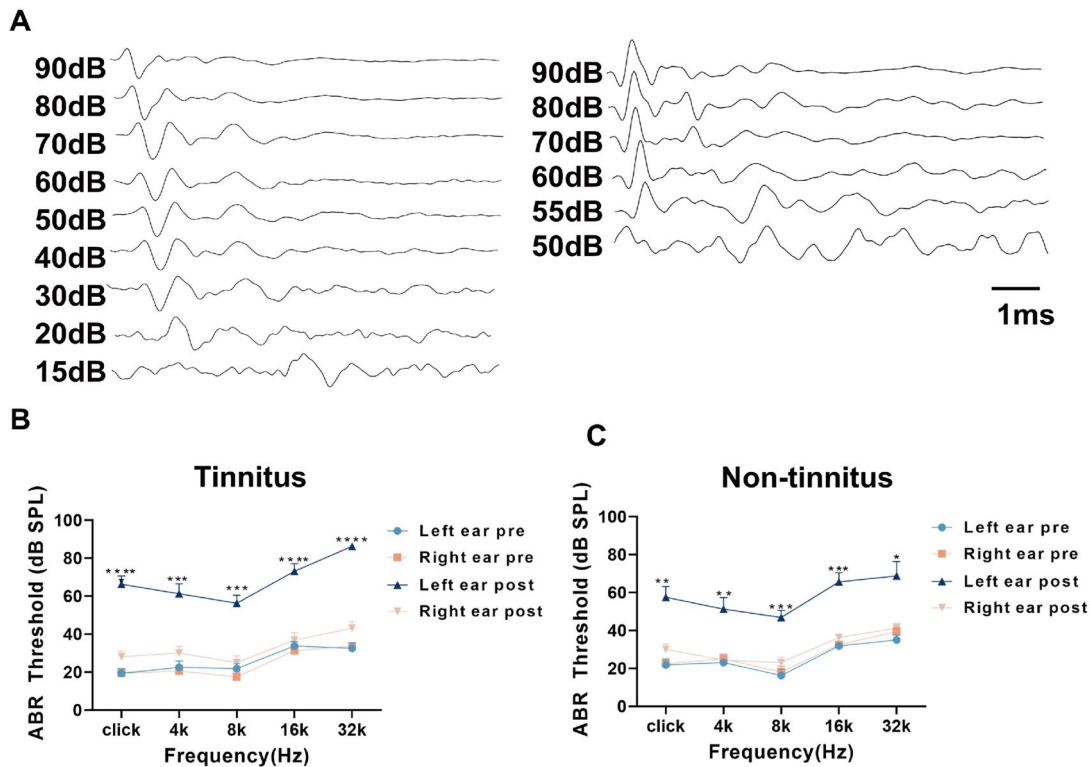


Figure 2. The ABR threshold of tinnitus group and non-tinnitus group. (A) Typical image showing the click-ABR threshold of the left ear before (left) and after the noise exposure (right). Summary graph showing ABR thresholds of bilateral ears before and 1 week after unilateral noise exposure in: (B) tinnitus and (C) non-tinnitus rats. In both the two groups, the ABR threshold in the left ear was significantly increased, but the hearing in the right ear was effectively protected in both groups. ($n=8$, **indicates $p < .01$, ***indicates $p < .001$, ****indicates $p < .0001$. Error bars indicate SEM.)

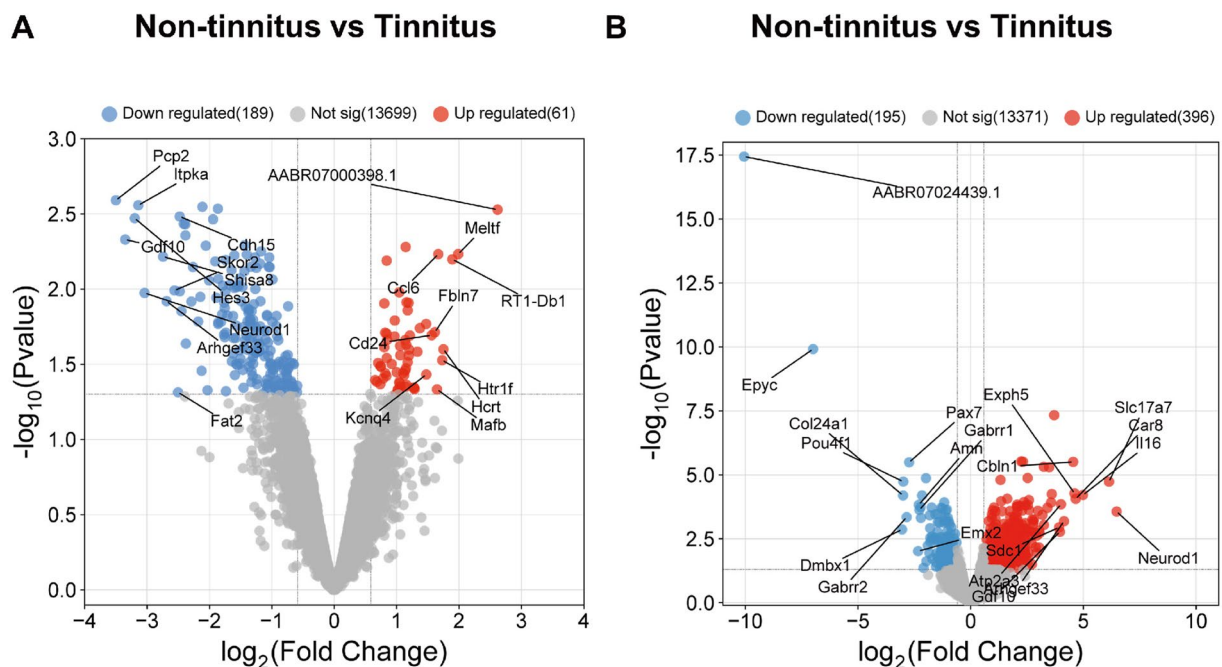


Figure 3. Identification of DEGs in the transcriptional level between tinnitus and non-tinnitus rats in DCN and IC. (A) Volcano plot of DEGs in DCN. (B) Volcano plot of DEGs in IC. Red dots represent upregulated genes and blue dots represent downregulated genes of tinnitus group compared with the non-tinnitus group ($n=3$).

Table 3. The top ten upregulated and downregulated DEGs in DCN.

| Up regulated genes | | | Down regulated genes | | |
|--------------------|----------|---------|----------------------|----------|---------|
| genes | log2FC | p-value | genes | log2FC | p-value |
| AABR07000398.1 | 2.616951 | .002963 | Pcp2 | -3.4988 | .002566 |
| Meltf | 1.986958 | .005852 | Gdf10 | -3.34906 | .004685 |
| RT1-Db1 | 1.892592 | .006338 | Hes3 | -3.19807 | .00338 |
| Hcrt | 1.750038 | .025154 | Itpka | -3.13995 | .002771 |
| Htr1f | 1.729877 | .029733 | Neurod1 | -3.03985 | .01061 |
| Ccl6 | 1.666695 | .005861 | Shisa8 | -2.74319 | .006086 |
| Mafb | 1.647114 | .046485 | Arhgef33 | -2.68747 | .012035 |
| Fbln7 | 1.612643 | .019355 | Skor2 | -2.56 | .010209 |
| Cd24 | 1.560991 | .020267 | Fat2 | -2.50272 | .048599 |
| Kcnq4 | 1.475378 | .036989 | Cdh15 | -2.47665 | .00329 |

Similarly, Go and KEGG enrichment analysis were also implemented in IC. Cilium movement, axoneme assembly, inner dynein arm assembly, microtubule-based movement, and axonemal dynein complex assembly were the top five terms in BP ontology (Figure 5A). Motile cilia constitute the most enriched CC process, followed by the axoneme, which is an integral component of the plasma membrane, cilium, and ciliary part (Figure 5B). The top five enriched terms in the MF process were calcium ion binding, RNA-DNA hybrid ribonuclease activity, extracellular matrix structural constituents, somatostatin receptor activity, and PH domain binding (Figure 5C). Meanwhile, the potential pathways identified from KEGG analysis were as follows: neuroactive ligand-receptor interactions, glutamatergic synapses, amphetamine addiction, nicotine addiction, and gastric acid secretion (Figure 5D).

3.4. Construction of the protein-protein interaction network and hub gene selection

The establishment of the PPI network involved the utilization of the STRING database [42,45]. We set the interaction score threshold of 0.900 (highest confidence) and 0.400 (medium confidence) respectively as the criterion. In the highest confidence level, the DCN network comprised 283 nodes and 43 edges, with an average node degree of 0.304 (Figure 6A). In the medium confidence level, the DCN network included 283 nodes and 401 edges, with an average node degree of 2.83 (Figure S3). Similarly, the IC network consisted of 585 nodes and 85 edges, with an average node degree of 0.291 in the highest confidence level (Figure 6B); and 585 nodes and 1595 edges in the medium confidence level, with an average node degree of 5.45 in the PPI network (Figure S4). After sorting the genes by betweenness centrality using the CytoNCA plugin, the Cytoscape software was utilized to visualize the top 30 highly connected genes in DCN and IC (Figure 6C,D). The hub genes identified from the DEGs

Table 4. The top ten upregulated and downregulated DEGs in IC.

| Up regulated genes | | | Down regulated genes | | |
|--------------------|----------|----------|----------------------|----------|----------|
| genes | log2FC | p-value | genes | log2FC | p-value |
| Neurod1 | 6.476636 | .000274 | AABR07024439.1 | -10.0544 | 3.65E-18 |
| Slc17a7 | 6.137731 | 1.86E-05 | Epyc | -6.99154 | 1.22E-10 |
| Il16 | 4.983716 | 6.14E-05 | Dmbx1 | -3.04417 | .001367 |
| Car8 | 4.661448 | 8.71E-05 | Col24a1 | -2.99925 | 6.42E-05 |
| Exph5 | 4.6079 | 5.31E-05 | Pou4f1 | -2.9888 | 1.85E-05 |
| Cbln1 | 4.549232 | 3.12E-06 | Gabbr2 | -2.84025 | .00045 |
| Arhgef33 | 4.141688 | .000653 | Pax7 | -2.72833 | 3.24E-06 |
| Atp2a3 | 4.008831 | .000142 | Emx2 | -2.33005 | .009639 |
| Gdf10 | 3.960473 | .001685 | Amn | -2.30027 | .000149 |
| Sdc1 | 3.920533 | .00114 | Gabbr1 | -2.27158 | .000234 |

of DCN and IC are listed in Table 5. In DCN, the hub genes include Calb1, Fos, Rgs8, Grid2, Hpcal4, Sdc1, Cacna1a, Gria1, and Itpr1. On the other hand, the hub genes for IC DEGs are Jup, Prkcg, Fos, Sdc1, Itgb4, Ush2a, Pax6, Kit, and Daw1.

3.5. Hub gene verification

The qPCR was used to evaluate the expression levels of the selected genes (Figure 7). In the DCN, among the tinnitus group, three hub genes—specifically Hpcal4 ($p < .05$, Figure 7E), Cacna1a ($p < .05$, Figure 7G), and Gria1 ($p < .05$, Figure 7H)—showed significant upregulation compared to the non-tinnitus group. Conversely, for other genes such as Calb1 (Figure 7A), Fos (Figure 7B), Grid2 (Figure 7C), Rgs8 (Figure 7D), Sdc1 (Figure 7F) and Itpr1 (Figure 7I), no statistical differences were observed between the two groups. On the other hand, no statistical differences were observed between the two groups of IC tissues for Jup (Figure 7J), Prkcg (Figure 7K), Fos (Figure 7L), Sdc1 (Figure 7M), Itgb4 (Figure 7N), Ush2a (Figure 7O), Pax6 (Figure 7P), Kit (Figure 7Q), and Daw1 (Figure 7R).

4. Discussion

In this experiment, we revealed some similarities in gene expression changes in the DCN and the IC in the noise-induced tinnitus rat models at the transcriptome level. The results indicated that there are several similarities of gene expression changes between DCN and IC. Firstly, c-fos was recognized as a hub gene in both the DCN and IC, serving as one of the immediate early genes extensively used as an indicator of neuronal activity, with its expression quickly increasing following neuronal stimulation. However, the qPCR experiment showed no disparity in the expression levels of c-fos in the two areas. This could be attributed to the fact that the tissue samples were collected one week after exposure to noise. Previous research indicates

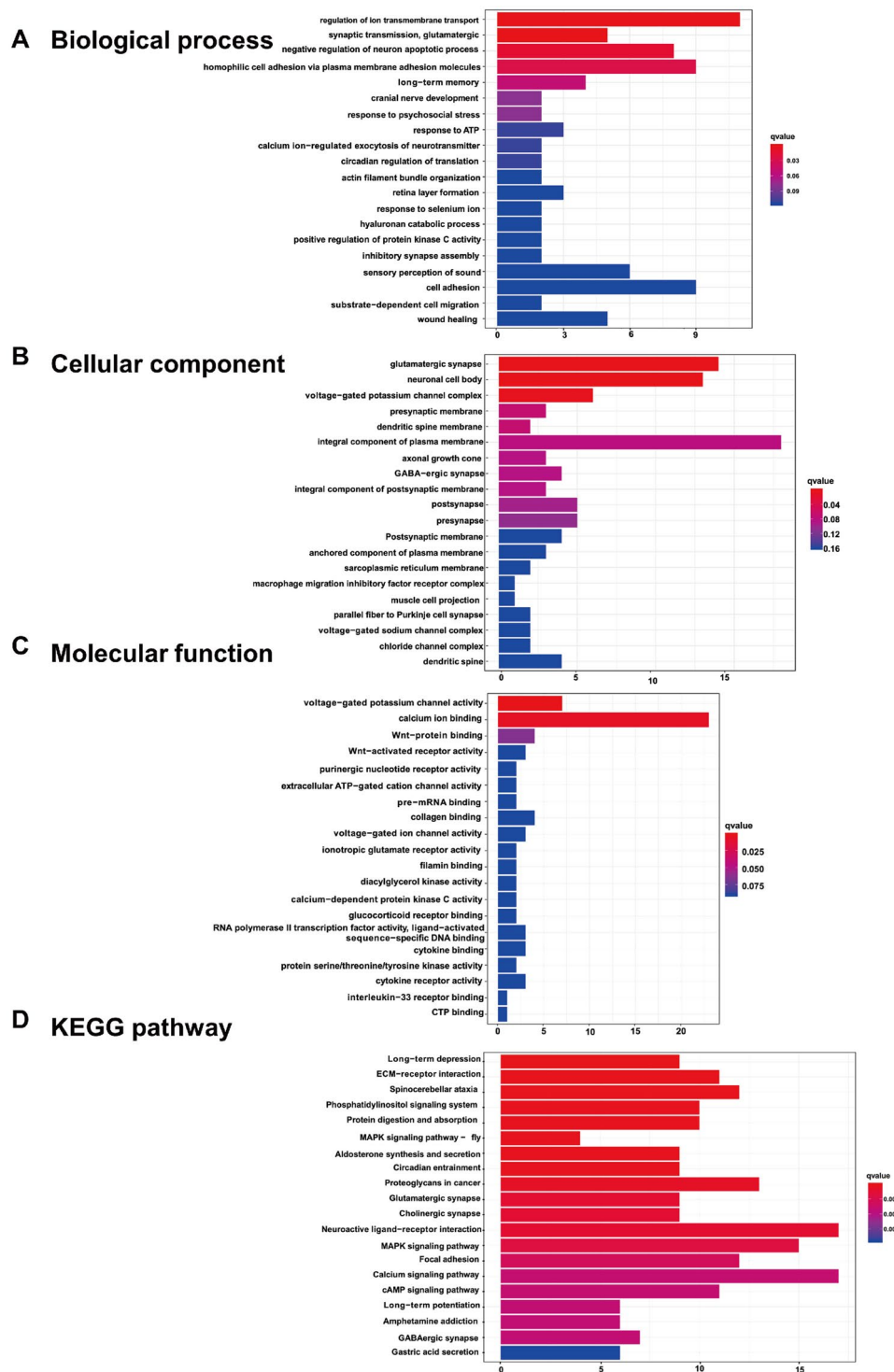


Figure 4. The enrichment analysis of DEGs in DCN. The top 20 GO functions for the DEGs (A-C), including (A) biological process, (B) cellular components and (C) molecular function; as well as (D) the enrichment map of KEGG analysis.

variations in the expression of immediate early genes, including *c-fos*, derived from samples collected 3 h after modeling with salicylate [46]. Secondly, the other DEGs are mainly enriched in pathways associated with increased neuronal excitability, particularly glutamatergic synapses. Glutamate is an excitatory neurotransmitter that plays an important role in the

central nervous system [47]. It can transmit excitatory signals between neurons, promoting neuronal excitation and information transmission. We may speculate that after 1 week of 116 dB, 16 kHz narrow-band noise exposure, the excitability of neurons in both the DCN and the IC show an upregulation trend, which is consistent with the conclusion drawn from previous

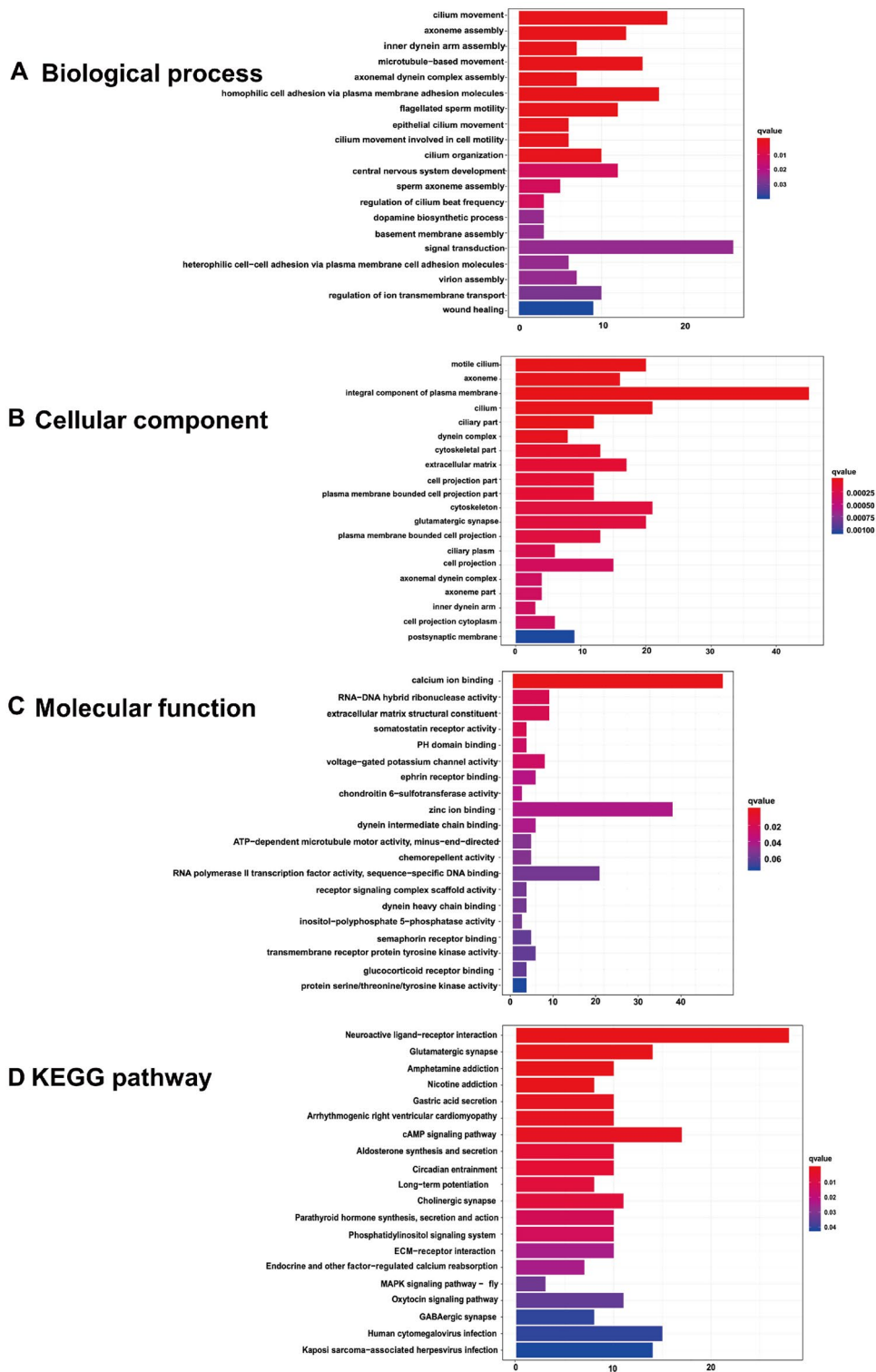


Figure 5. The enrichment analysis of DEGs in IC. The top 20 GO functions for the DEGs (A-C), including (A)biological process, (B) cellular components and (C) molecular function; as well as (D) the enrichment map of KEGG analysis.

studies regarding hyperactivity in both DCN and IC [48–50].

Moreover, we have detected significant upregulation of three core genes – *Hpcal4*, *Gria1*, and *Cacna1a* – in the DCN tissue of rats with tinnitus when contrasted with the non-tinnitus rats, and further

validation was obtained through qPCR experiments. This upregulation strongly implies that these genes likely have a crucial involvement in the initiation and progression of tinnitus. *Hpcal4*, a member of the visinin-like calcium binding proteins superfamily, is responsible for encoding a gene that is intricately

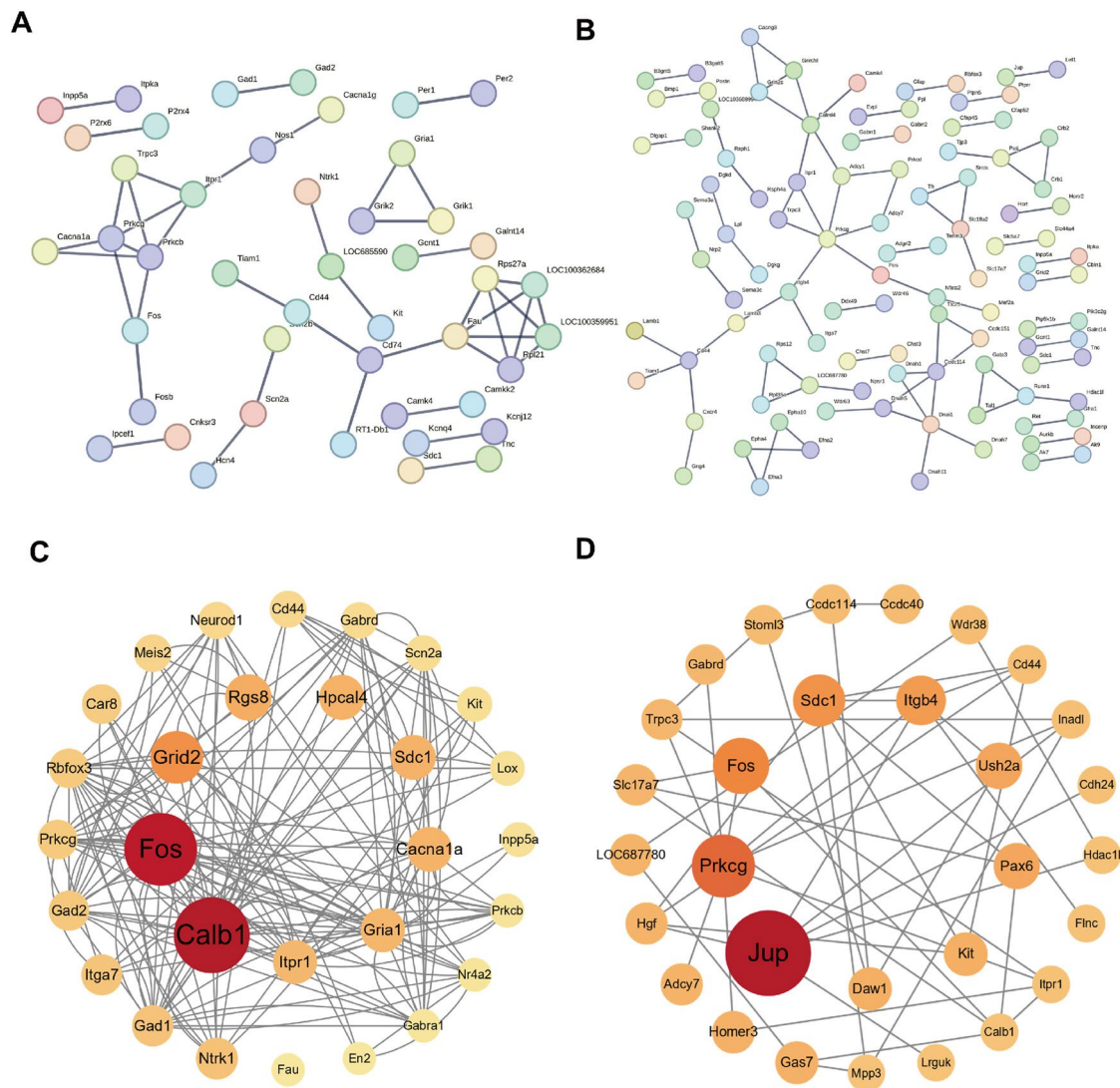


Figure 6. The protein–protein interaction (PPI) network, showing (A and B) the string interactions between the DEGs and (C and D) hub genes ranked by betweenness centrality in DCN and IC. In the network, nodes represent genes and edges represent the interactions between the nodes.

Table 5. Top 9 in network string ranked by BC in DCN and IC.

| Ranked by BC | DCN | | IC | |
|--------------|-----------|-----------|-----------|------------|
| | Gene name | Score | Gene name | Score |
| 1 | Calb1 | 5908.408 | Jup | 29,226.781 |
| 2 | Fos | 5542.9453 | Prkcg | 18,242.19 |
| 3 | Grid2 | 3293.2832 | Fos | 14,816.118 |
| 4 | Rgs8 | 2587.2534 | Sdc1 | 12,864.146 |
| 5 | Hpcal4 | 2434.896 | Itgb4 | 11,662.154 |
| 6 | Sdc1 | 2420.3457 | Ush2a | 10,049.483 |
| 7 | Cacna1a | 2405.07 | Pax6 | 9919.142 |
| 8 | Gria1 | 2336.574 | Kit | 8717.504 |
| 9 | Itpr1 | 2303.5435 | Daw1 | 8562.324 |

involved in calcium-binding proteins and plays a crucial role in the inactivation of Cav2.1 channels [51]. Interestingly, another core gene -Cacna1a- encodes the Cav2.1 α 1 subunit of the P/Q-type voltage-gated Ca^{2+} channel. Therefore, we have reason to speculate

that Cav2.1 channels may play a role in the occurrence of tinnitus, which are located in somatodendritic membranes and presynaptic terminals throughout the brain and play a pivotal role in triggering neurotransmitter release and synaptic plasticity by facilitating Ca^{2+} influx [52–54]. In a carrying a familial hemiplegic migraine type 1 mutation mice study, which is characterized by increased neuronal P/Q-type current, the authors clarified the increased strength of cortical excitatory synaptic transmission due to increased action-potential-evoked Ca^{2+} influx through presynaptic Cav2.1 channels [55,56]. And it has also been illustrated that the regulation of synaptic transmission contributed to the central excitability changes after hearing loss [57]. Additionally, Gria1 is responsible for encoding the GluA1 subunit of the AMPA subtype of glutamate receptors [58]. In another study, it was also

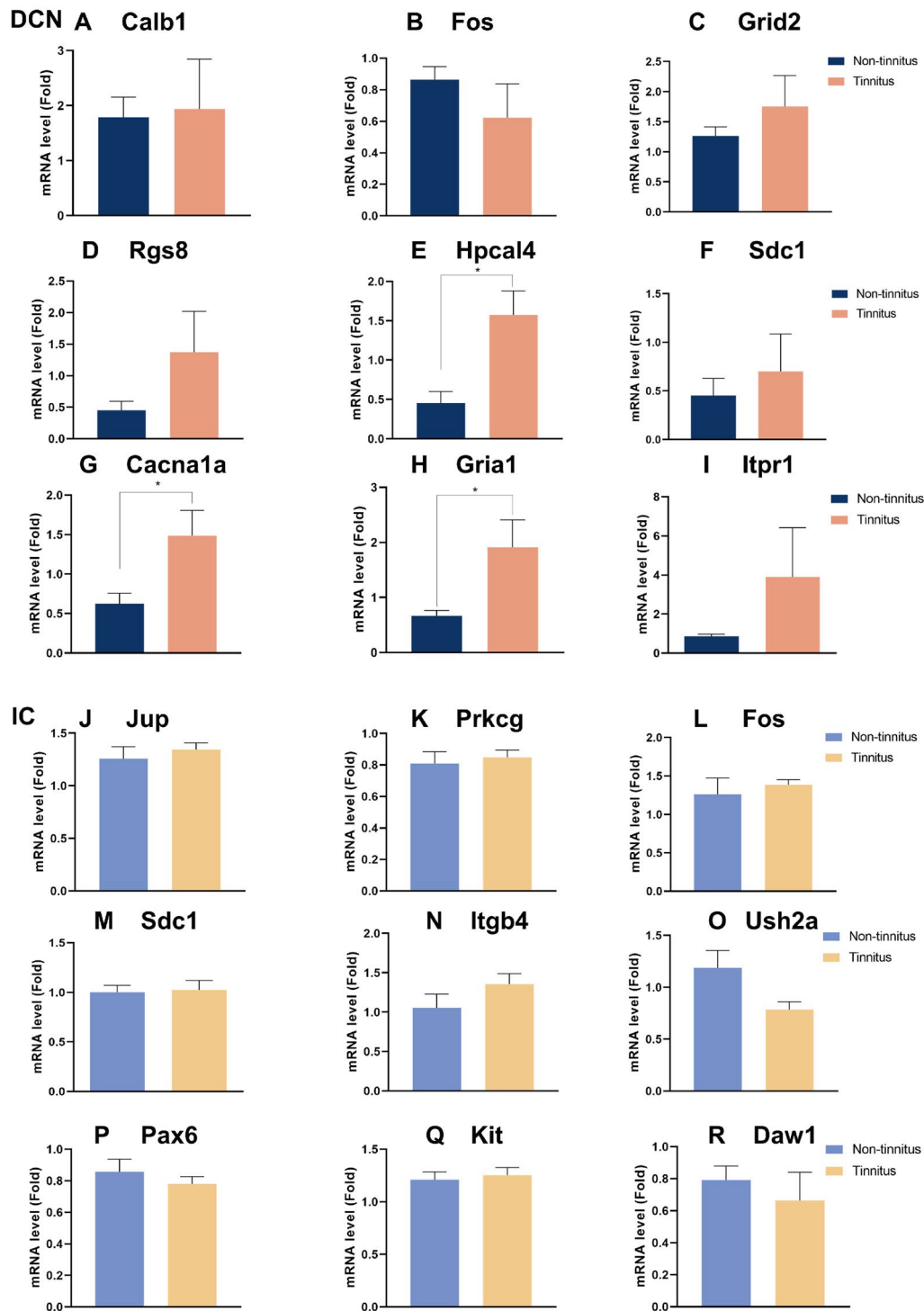


Figure 7. Confirmation of hub genes. qPCR test of 9 hub genes in DCN and IC, including (A) Calb1, (B) Fos, (C) Grid2, (D) Rgs8, (E) Hpcal4 ($p = .0111$), (F) Sdc1, (G) Cacna1a ($p = .0369$), (H) Gria1 ($p = .0402$) and (I) Itpr1 in DCN; as well as (J) Jup, (K) Prkcg, (L) Fos, (M) Sdc1, (N) Itgb4, (O) Ush2a, (P) Pax6, (Q) Kit, and (R) Daw1 in IC. Blue represents the non-tinnitus group and orange represents the tinnitus group. ($n = 5$, * indicates $p < .05$).

reported that Gria2 level was increased after unilateral hearing loss, which may contribute to the excitatory/inhibitory unbalance in auditory center [59]. And it is well-known that synaptic excitatory/inhibitory balance plays an important role in the mechanism of tinnitus development [60].

In general, neuronal plasticity plays an important role in the neuronal hyperactivity related to tinnitus, which could be attributed to the plasticity of intrinsic excitability of neurons and synaptic transmission [61]. The former is one example of neuronal plasticity, which indicates changes in how a neuron reacts to

incoming information [62]. Research suggests that the intrinsic excitability of neurons is often associated with potassium channels found on the cell surface in DCN [63]. In the current study, the DEGs in DCN are not only enriched in signaling pathways related to the intrinsic excitability of DCN neurons, such as voltage-gated potassium channel activity being the first enriched term in the MF category (Figure 4C), but also enriched in pathways associated with synaptic transmission, such as synaptic transmission in biological process enrichment analysis, as well as glutamatergic synapse, presynaptic membrane, and dendritic spine membrane glutamatergic synapse in cellular component enrichment analysis. In contrast, the pathways enriched by DEGs in the IC are rarely related to the synaptic transmission characteristics of neurons. This leads us to speculate that the increased excitability of IC neurons is closely related to the plasticity changes of DCN neurons.

Moreover, this speculation has also been more or less confirmed in previous studies. The phenomenon of increased excitability of IC neurons as suggested by previous electrophysiological experiments is largely attributed to the increased excitatory signal input from the DCN [64]. Previous research results also indicate that although the excitability of neurons in both the DCN and IC shows an increasing trend, the trend of increased excitability in IC neurons is significantly weaker compared to that in DCN neurons [31]. This further suggests that the increase in excitability of IC neurons may largely depend on the excitatory signal input from the DCN.

It is undeniable that there are several limitations in our study. Firstly, we cannot completely rule out other alternative explanations for the increased excitability of IC neurons besides receiving the exciting projections from DCN. For example, the heightened activity in the IC could potentially arise from a higher-level source, such as the auditory cortex, which may transmit signals to the IC and DCN through top-down corticofugal pathways [65]. It is well-established that descending fibers originating in laminae V of the primary auditory cortex project to the IC and DCN [66,67]. Secondly, we only validated the expression differences of hub genes at the transcriptomic level, without confirmation at the protein level, and also did not further investigate the effects of hub gene overexpression or knockdown on neuronal excitability at the cellular functional level. Additional research is needed to ascertain whether these genes can be clinically translated into viable targets for tinnitus treatment.

In summary, we utilized transcriptome sequencing technology to examine the gene expression levels in

the DCN and IC of a noise-induced tinnitus rat model. Our findings reveal an enrichment of DEGs associated with pathways linked to alterations in neuronal excitability within the DCN and IC when comparing the tinnitus group to the non-tinnitus group. This indicates an increased trend in neuronal excitability within both the DCN and IC in the tinnitus model rats. Additionally, the enriched signaling pathways related to changes in synaptic plasticity in the differentially expressed genes within the DCN suggest that the excitability changes may propagate to IC.

Authors contributions

S Yang, F Wang, and X Xue designed the study. X Xue and P Liu executed the experiments. C Zhang, and Z Ding analyzed the data. Y Jiang, L Wang, and W Shen performed the writing of the current manuscript. S Yang, F Wang, and X Xue revised the manuscript.

Disclosure statement

The authors declare that the research was conducted in the absence of any commercial or financial relationships that could be construed as a potential conflict of interest.

Funding

This work was supported by the National Clinical Research Center for Otolaryngologic Diseases, Beijing 100853, PR China.

ORCID

Xinmiao Xue  <http://orcid.org/0000-0002-0005-4207>

Data availability statement

The raw data supporting the conclusions of this article will be made available by the authors, without undue reservation.

References

- [1] Sedley W, Friston KJ, Gander PE, et al. An integrative tinnitus model based on sensory precision. *Trends Neurosci.* 2016;39(12):799–812. doi: [10.1016/j.tins.2016.10.004](https://doi.org/10.1016/j.tins.2016.10.004).
- [2] Sedley W, Alter K, Gander PE, et al. Exposing pathological sensory predictions in tinnitus using auditory intensity deviant evoked responses. *J Neurosci.* 2019;39(50):10096–10103. doi: [10.1523/jneurosci.1308-19.2019](https://doi.org/10.1523/jneurosci.1308-19.2019).
- [3] Lan L, Chen Y-C, Shang S, et al. Topological features of limbic dysfunction in chronicity of tinnitus with intact hearing: new hypothesis for ‘noise-cancellation’ mechanism. *Prog Neuropsychopharmacol Biol Psychiatry.* 2022;113:110459. doi: [10.1016/j.pnpbp.2021.110459](https://doi.org/10.1016/j.pnpbp.2021.110459).
- [4] Zeng FG. Tinnitus and hyperacusis: central noise, gain and variance. *Curr Opin Physiol.* 2020;18:123–129. doi: [10.1016/j.cophys.2020.10.009](https://doi.org/10.1016/j.cophys.2020.10.009).

- [5] Krauss P, Tziridis K, Metzner C, et al. Stochastic resonance controlled upregulation of internal noise after hearing loss as a putative cause of tinnitus-related neuronal hyperactivity. *Front Neurosci.* 2016;10:597. doi: [10.3389/fnins.2016.00597](https://doi.org/10.3389/fnins.2016.00597).
- [6] Sedley W. Tinnitus: does gain explain? *Neuroscience.* 2019;407:213–228. doi: [10.1016/j.neuroscience.2019.01.027](https://doi.org/10.1016/j.neuroscience.2019.01.027).
- [7] Schilling A, Sedley W, Gerum R, et al. Predictive coding and stochastic resonance as fundamental principles of auditory phantom perception. *Brain.* 2023;146(12):4809–4825. doi: [10.1093/brain/awad255](https://doi.org/10.1093/brain/awad255).
- [8] Hazell JW, Jastreboff PJ, Tinnitus I. Auditory mechanisms: a model for tinnitus and hearing impairment. *J Otolaryngol.* 1990;19:1–5.
- [9] Schaette R, McAlpine D. Tinnitus with a normal audiogram: physiological evidence for hidden hearing loss and computational model. *J Neurosci.* 2011;31(38):13452–13457. doi: [10.1523/jneurosci.2156-11.2011](https://doi.org/10.1523/jneurosci.2156-11.2011).
- [10] Bajin MD, Dahm V, Lin VYW. Hidden hearing loss: current concepts. *Curr Opin Otolaryngol Head Neck Surg.* 2022;30(5):321–325. doi: [10.1097/moo.0000000000000824](https://doi.org/10.1097/moo.0000000000000824).
- [11] Tziridis K, Forster J, Buchheidt-Dörfler I, et al. Tinnitus development is associated with synaptopathy of inner hair cells in *Mongolian gerbils*. *Eur J Neurosci.* 2021;54(3):4768–4780. doi: [10.1111/ejn.15334](https://doi.org/10.1111/ejn.15334).
- [12] Tziridis K, Schulze H. Preventive effects of ginkgo-extract EGb 761(®) on noise trauma-induced cochlear synaptopathy. *Nutrients.* 2022;14(15):3015. doi: [10.3390/nu14153015](https://doi.org/10.3390/nu14153015).
- [13] Sly DJ, Heffer LF, White MW, et al. Deafness alters auditory nerve fibre responses to cochlear implant stimulation. *Eur J Neurosci.* 2007;26(2):510–522. doi: [10.1111/j.1460-9568.2007.05678.x](https://doi.org/10.1111/j.1460-9568.2007.05678.x).
- [14] Schaette R, Kempter R. Predicting tinnitus pitch from patients' audiograms with a computational model for the development of neuronal hyperactivity. *J Neurophysiol.* 2009;101(6):3042–3052. doi: [10.1152/jn.91256.2008](https://doi.org/10.1152/jn.91256.2008).
- [15] Noreña AJ. An integrative model of tinnitus based on a central gain controlling neural sensitivity. *Neurosci Biobehav Rev.* 2011;35(5):1089–1109. doi: [10.1016/j.neubiorev.2010.11.003](https://doi.org/10.1016/j.neubiorev.2010.11.003).
- [16] Wu C, Martel DT, Shore SE. Increased synchrony and bursting of dorsal cochlear nucleus fusiform cells correlate with tinnitus. *J Neurosci.* 2016;36(6):2068–2073. doi: [10.1523/jneurosci.3960-15.2016](https://doi.org/10.1523/jneurosci.3960-15.2016).
- [17] Malfatti T, Ciralli B, Hilscher MM, et al. Decreasing dorsal cochlear nucleus activity ameliorates noise-induced tinnitus perception in mice. *BMC Biol.* 2022;20(1):102. doi: [10.1186/s12915-022-01288-1](https://doi.org/10.1186/s12915-022-01288-1).
- [18] Martel DT, Pardo-Garcia TR, Shore SE. Dorsal cochlear nucleus fusiform-cell plasticity is altered in salicylate-induced tinnitus. *Neuroscience.* 2019;407:170–181. doi: [10.1016/j.neuroscience.2018.08.035](https://doi.org/10.1016/j.neuroscience.2018.08.035).
- [19] Brozoski TJ, Wisner KW, Sybert LT, et al. Bilateral dorsal cochlear nucleus lesions prevent acoustic-trauma induced tinnitus in an animal model. *J Assoc Res Otolaryngol.* 2012;13(1):55–66. doi: [10.1007/s10162-011-0290-3](https://doi.org/10.1007/s10162-011-0290-3).
- [20] Brozoski TJ, Bauer CA. The effect of dorsal cochlear nucleus ablation on tinnitus in rats. *Hear Res.* 2005;206(1-2):227–236. doi: [10.1016/j.heares.2004.12.013](https://doi.org/10.1016/j.heares.2004.12.013).
- [21] Luo H, Pace E, Zhang X, et al. Blast-induced tinnitus and spontaneous activity changes in the rat inferior colliculus. *Neurosci Lett.* 2014;580:47–51. doi: [10.1016/j.neulet.2014.07.041](https://doi.org/10.1016/j.neulet.2014.07.041).
- [22] Ropp TJ, Tiedemann KL, Young ED, et al. Effects of unilateral acoustic trauma on tinnitus-related spontaneous activity in the inferior colliculus. *J Assoc Res Otolaryngol.* 2014;15(6):1007–1022. doi: [10.1007/s10162-014-0488-2](https://doi.org/10.1007/s10162-014-0488-2).
- [23] Kalappa BI, Brozoski TJ, Turner JG, et al. Single unit hyperactivity and bursting in the auditory thalamus of awake rats directly correlates with behavioural evidence of tinnitus. *J Physiol.* 2014;592(22):5065–5078. doi: [10.1113/jphysiol.2014.278572](https://doi.org/10.1113/jphysiol.2014.278572).
- [24] Luo H, Pace E, Zhang J. Blast-induced tinnitus and hyperactivity in the auditory cortex of rats. *Neuroscience.* 2017;340:515–520. doi: [10.1016/j.neuroscience.2016.11.014](https://doi.org/10.1016/j.neuroscience.2016.11.014).
- [25] Eggermont JJ. Separate auditory pathways for the induction and maintenance of tinnitus and hyperacusis? *Prog Brain Res.* 2021;260:101–127. doi: [10.1016/bs.pbr.2020.01.006](https://doi.org/10.1016/bs.pbr.2020.01.006).
- [26] Bauer CA, Turner JG, Caspary DM, et al. Tinnitus and inferior colliculus activity in chinchillas related to three distinct patterns of cochlear trauma. *J Neurosci Res.* 2008;86(11):2564–2578. doi: [10.1002/jnr.21699](https://doi.org/10.1002/jnr.21699).
- [27] Niu Y, Kumaraguru A, Wang R, et al. Hyperexcitability of inferior colliculus neurons caused by acute noise exposure. *J Neurosci Res.* 2013;91(2):292–299. doi: [10.1002/jnr.23152](https://doi.org/10.1002/jnr.23152).
- [28] Sturm JJ, Zhang-Hooks YX, Roos H, et al. Noise trauma-induced behavioral gap detection deficits correlate with reorganization of excitatory and inhibitory local circuits in the inferior colliculus and are prevented by acoustic enrichment. *J Neurosci.* 2017;37(26):6314–6330. doi: [10.1523/jneurosci.0602-17.2017](https://doi.org/10.1523/jneurosci.0602-17.2017).
- [29] Berger JI, Coomber B. Tinnitus-related changes in the inferior colliculus. *Front Neurol.* 2015;6:61. doi: [10.3389/fneur.2015.00061](https://doi.org/10.3389/fneur.2015.00061).
- [30] Berger JI, Coomber B, Wells TT, et al. Changes in the response properties of inferior colliculus neurons relating to tinnitus. *Front Neurol.* 2014;5:203. doi: [10.3389/fneur.2014.00203](https://doi.org/10.3389/fneur.2014.00203).
- [31] Manzoor NF, Gao Y, Licari F, et al. Comparison and contrast of noise-induced hyperactivity in the dorsal cochlear nucleus and inferior colliculus. *Hear Res.* 2013;295(1-2):114–123. doi: [10.1016/j.heares.2012.04.003](https://doi.org/10.1016/j.heares.2012.04.003).
- [32] Koch M. Sensorimotor gating changes across the estrous cycle in female rats. *Physiol Behav.* 1998;64(5):625–628. doi: [10.1016/s0031-9384\(98\)00098-5](https://doi.org/10.1016/s0031-9384(98)00098-5).
- [33] Longenecker RJ, Kristaponyte I, Nelson GL, et al. Addressing variability in the acoustic startle reflex for accurate gap detection assessment. *Hear Res.* 2018;363:119–135. doi: [10.1016/j.heares.2018.03.013](https://doi.org/10.1016/j.heares.2018.03.013).
- [34] Arifin WN, Zahiruddin WM. Sample size calculation in animal studies using resource equation approach. *Malays J Med Sci.* 2017;24(5):101–105. doi: [10.21315/mjms2017.24.5.11](https://doi.org/10.21315/mjms2017.24.5.11).
- [35] Lundt A, Henseler C, Wormuth C, et al. Gender specific click and tone burst evoked ABR datasets from mice lacking the Ca(v)2.3 R-type voltage-gated calcium channel. *Data Brief.* 2018;21:1263–1266. doi: [10.1016/j.dib.2018.10.056](https://doi.org/10.1016/j.dib.2018.10.056).
- [36] Wang M-L, Song Y, Liu J-X, et al. Role of the caudate-putamen nucleus in sensory gating in induced tinnitus in rats. *Neural Regen Res.* 2021;16(11):2250–2256. doi: [10.4103/1673-5374.310692](https://doi.org/10.4103/1673-5374.310692).
- [37] Dehmel S, Pradhan S, Koehler S, et al. Noise overexposure alters long-term somatosensory-auditory processing in the dorsal cochlear nucleus—possible basis for tinnitus-related hyperactivity? *J Neurosci.* 2012;32(5):1660–1671. doi: [10.1523/jneurosci.4608-11.2012](https://doi.org/10.1523/jneurosci.4608-11.2012).

- [38] Kraus KS, Mitra S, Jimenez Z, et al. Noise trauma impairs neurogenesis in the rat hippocampus. *Neuroscience*. 2010;167(4):1216–1226. doi: [10.1016/j.neuroscience.2010.02.071](https://doi.org/10.1016/j.neuroscience.2010.02.071).
- [39] Longenecker RJ, Galazyuk AV. Development of tinnitus in CBA/CaJ mice following sound exposure. *J Assoc Res Otolaryngol*. 2011;12(5):647–658. doi: [10.1007/s10162-011-0276-1](https://doi.org/10.1007/s10162-011-0276-1).
- [40] Longenecker RJ, Chonko KT, Maricich SM, et al. Age effects on tinnitus and hearing loss in CBA/CaJ mice following sound exposure. *Springerplus*. 2014;3(1):542. doi: [10.1186/2193-1801-3-542](https://doi.org/10.1186/2193-1801-3-542).
- [41] Turner JG, Brozoski TJ, Bauer CA, et al. Gap detection deficits in rats with tinnitus: a potential novel screening tool. *Behav Neurosci*. 2006;120(1):188–195. doi: [10.1037/0735-7044.120.1.188](https://doi.org/10.1037/0735-7044.120.1.188).
- [42] Szklarczyk D, Gable AL, Lyon D, et al. STRING v11: protein-protein association networks with increased coverage, supporting functional discovery in genome-wide experimental datasets. *Nucleic Acids Res*. 2019;47(D1):D607–d613. doi: [10.1093/nar/gky1131](https://doi.org/10.1093/nar/gky1131).
- [43] Zeidán-Chuliá F, Gürsoy M, Neves de Oliveira B-H, et al. A systems biology approach to reveal putative host-derived biomarkers of periodontitis by network topology characterization of MMP-REDOX/NO and apoptosis integrated pathways. *Front Cell Infect Microbiol*. 2015;5:102. doi: [10.3389/fcimb.2015.00102](https://doi.org/10.3389/fcimb.2015.00102).
- [44] Tang Y, Li M, Wang J, et al. CytoNCA: a cytoscape plugin for centrality analysis and evaluation of protein interaction networks. *Biosystems*. 2015;127:67–72. doi: [10.1016/j.biosystems.2014.11.005](https://doi.org/10.1016/j.biosystems.2014.11.005).
- [45] Szklarczyk D, Morris JH, Cook H, et al. The STRING database in 2017: quality-controlled protein-protein association networks, made broadly accessible. *Nucleic Acids Res*. 2017;45(D1):D362–d368. doi: [10.1093/nar/gkw937](https://doi.org/10.1093/nar/gkw937).
- [46] Montazeri K, Farhadi M, Akbarnejad Z, et al. Acoustic and optoacoustic stimulations in auditory brainstem response test in salicylate induced tinnitus. *Sci Rep*. 2023;13(1):11930. doi: [10.1038/s41598-023-39033-5](https://doi.org/10.1038/s41598-023-39033-5).
- [47] Brosnan JT, Brosnan ME. Glutamate: a truly functional amino acid. *Amino Acids*. 2013;45(3):413–418. doi: [10.1007/s00726-012-1280-4](https://doi.org/10.1007/s00726-012-1280-4).
- [48] Heeringa AN, Wu C, Chung C, et al. Glutamatergic projections to the cochlear nucleus are redistributed in tinnitus. *Neuroscience*. 2018;391:91–103. doi: [10.1016/j.neuroscience.2018.09.008](https://doi.org/10.1016/j.neuroscience.2018.09.008).
- [49] Basta D, Götze R, Gröschel M, et al. Bilateral changes of spontaneous activity within the central auditory pathway upon chronic unilateral intracochlear electrical stimulation. *Otol Neurotol*. 2015;36(10):1759–1765. doi: [10.1097/mao.0000000000000894](https://doi.org/10.1097/mao.0000000000000894).
- [50] Tan HT, Smith PF, Zheng Y. Time-dependent effects of acoustic trauma and tinnitus on extracellular levels of amino acids in the inferior colliculus of rats. *Hear Res*. 2024;443:108948. doi: [10.1016/j.heares.2024.108948](https://doi.org/10.1016/j.heares.2024.108948).
- [51] Lautermilch NJ, Few AP, Scheuer T, et al. Modulation of CaV2.1 channels by the neuronal calcium-binding protein visinin-like protein-2. *J Neurosci*. 2005;25(30):7062–7070. doi: [10.1523/jneurosci.0447-05.2005](https://doi.org/10.1523/jneurosci.0447-05.2005).
- [52] Mori Y, Friedrich T, Kim MS, et al. Primary structure and functional expression from complementary DNA of a brain calcium channel. *Nature*. 1991;350(6317):398–402. doi: [10.1038/350398a0](https://doi.org/10.1038/350398a0).
- [53] Nanou E, Catterall WA. Calcium channels, synaptic plasticity, and neuropsychiatric disease. *Neuron*. 2018;98(3):466–481. doi: [10.1016/j.neuron.2018.03.017](https://doi.org/10.1016/j.neuron.2018.03.017).
- [54] Westenbroek RE, Sakurai T, Elliott EM, et al. Immunochemical identification and subcellular distribution of the alpha 1A subunits of brain calcium channels. *J Neurosci*. 1995;15(10):6403–6418. doi: [10.1523/jneurosci.15-10-06403.1995](https://doi.org/10.1523/jneurosci.15-10-06403.1995).
- [55] Tottene A, Conti R, Fabbro A, et al. Enhanced excitatory transmission at cortical synapses as the basis for facilitated spreading depression in Ca(v)2.1 knockin migraine mice. *Neuron*. 2009;61(5):762–773. doi: [10.1016/j.neuron.2009.01.027](https://doi.org/10.1016/j.neuron.2009.01.027).
- [56] Pietrobon D. Insights into migraine mechanisms and CaV2.1 calcium channel function from mouse models of familial hemiplegic migraine. *J Physiol*. 2010;588(Pt 11):1871–1878. doi: [10.1113/jphysiol.2010.188003](https://doi.org/10.1113/jphysiol.2010.188003).
- [57] Pilati N, Ison MJ, Barker M, et al. Mechanisms contributing to central excitability changes during hearing loss. *Proc Natl Acad Sci U S A*. 2012;109(21):8292–8297. doi: [10.1073/pnas.1116981109](https://doi.org/10.1073/pnas.1116981109).
- [58] Salpietro V, Dixon CL, Guo H, et al. AMPA receptor GluA2 subunit defects are a cause of neurodevelopmental disorders. *Nat Commun*. 2019;10(1):3094. doi: [10.1038/s41467-019-10910-w](https://doi.org/10.1038/s41467-019-10910-w).
- [59] Balamam P, Hackett TA, Polley DB. Synergistic transcriptional changes in AMPA and GABA(A) receptor genes support compensatory plasticity following unilateral hearing loss. *Neuroscience*. 2019;407:108–119. doi: [10.1016/j.neuroscience.2018.08.023](https://doi.org/10.1016/j.neuroscience.2018.08.023).
- [60] Irvine DRF. Plasticity in the auditory system. *Hear Res*. 2018;362:61–73. doi: [10.1016/j.heares.2017.10.011](https://doi.org/10.1016/j.heares.2017.10.011).
- [61] Wu C, Stefanescu RA, Martel DT, et al. Tinnitus: maladaptive auditory-somatosensory plasticity. *Hear Res*. 2016;334:20–29. doi: [10.1016/j.heares.2015.06.005](https://doi.org/10.1016/j.heares.2015.06.005).
- [62] Yousuf H, Ehlers VL, Sehgal M, et al. Modulation of intrinsic excitability as a function of learning within the fear conditioning circuit. *Neurobiol Learn Mem*. 2020;167:107132. doi: [10.1016/j.nlm.2019.107132](https://doi.org/10.1016/j.nlm.2019.107132).
- [63] Kanold PO, Manis PB. A physiologically based model of discharge pattern regulation by transient K⁺ currents in cochlear nucleus pyramidal cells. *J Neurophysiol*. 2001;85(2):523–538. doi: [10.1152/jn.2001.85.2.523](https://doi.org/10.1152/jn.2001.85.2.523).
- [64] Manzoor NF, Licari FG, Klapchar M, et al. Noise-induced hyperactivity in the inferior colliculus: its relationship with hyperactivity in the dorsal cochlear nucleus. *J Neurophysiol*. 2012;108(4):976–988. doi: [10.1152/jn.00833.2011](https://doi.org/10.1152/jn.00833.2011).
- [65] Tziridis K, Ahlf S, Jeschke M, et al. Noise trauma induced neural plasticity throughout the auditory system of *Mongolian gerbils*: differences between tinnitus developing and non-developing animals. *Front Neurol*. 2015;6:22. doi: [10.3389/fneur.2015.00022](https://doi.org/10.3389/fneur.2015.00022).
- [66] Meltzer NE, Ryugo DK. Projections from auditory cortex to cochlear nucleus: a comparative analysis of rat and mouse. *Anat Rec A Discov Mol Cell Evol Biol*. 2006;288(4):397–408. doi: [10.1002/ar.a.20300](https://doi.org/10.1002/ar.a.20300).
- [67] Schofield BR, Coomes DL. Pathways from auditory cortex to the cochlear nucleus in guinea pigs. *Hear Res*. 2006;216-217:81–89. doi: [10.1016/j.heares.2006.01.004](https://doi.org/10.1016/j.heares.2006.01.004).